High Resolution Airborne Gravity Gradiometry, Electromagnetic and Magnetic data for Geothermal Assessment

Craig Annison
Xcalibur Multiphysics
craig.annison@xcaliburmp.com

Jurriaan Feijth
Xcalibur Multiphysics
jurriaan.feijth@xcaliburmp.com

SUMMARY

Advances in airborne technologies has enabled rapid and efficient acquisition of high-resolution gravity, electromagnetic and magnetic datasets for geothermal assessment.

HeliFalcon airborne gravity gradiometry (AGG) can acquire high quality gravity data in most terrains, which is ideal for detailed litho-structural mapping of tectonic, volcanic and igneous features (faults, lava domes, lava flows, intrusives, calderas, basins, sub-basins), and general geology.

Helitem time-domain helicopter electromagnetics (AEM), operating at transmitter frequencies as low as 6.25Hz, provides enhanced exploration depth, and AEM data ideal for mapping subsurface resistivity distribution in 2D and 3D (and particularly low-resistivity clay-caps related to hydrothermal alteration), aquifers and lithological distribution. Resistivity depth slices and 3D iso-surfaces are used to image low resistivity zones, giving information on fluid sources, pathways, conduits at fault intersections, and alteration.

Magnetic data, acquired simultaneously with the AGG and/or AEM data, provides complementary information for the mapping applications above, and can also map areas of magnetite destruction due to hydrothermal alteration.

A geothermal case history from Japan is used to demonstrate how high-resolution airborne gravity, electromagnetic and magnetic datasets, can benefit geothermal assessment.

Key words: geothermal, airborne, gravity gradiometry, electromagnetics, magnetics

INTRODUCTION

In 2015 and 2016, airborne gravity gradiometry, electromagnetic and magnetic surveys were undertaken for Japan Oil, Gas and Metals National Corporation (JOGMEC) in rugged terrain in the Musadake-Teshikaga area of NE Hokkaido, Japan.

The surveys were part of a larger project titled “The Wide Area Airborne Geophysical Surveys for the Potential Evaluation of Geothermal Energy” which has undertaken airborne gravity gradiometry, electromagnetic and magnetic surveys for JOGMEC each year since 2013 for the evaluation of geothermal resources and to promote geothermal development.

This paper describes the airborne geophysical technologies used, the datasets acquired, the integrated interpretation, and the implications for geothermal prospectivity.

The AIRBORNE GEOPHYSICAL TECHNOLOGIES

HeliFalcon Airborne Gravity Gradiometry

Falcon AGG technology was developed in a collaborative project between BHP Billiton and Lockheed Martin which adapted US Navy technology into practical instrumentation for deployment in light fixed wing and helicopter aircraft. HeliFalcon is the only AGG system operable on a helicopter, and capable survey in rugged terrain.

Lee (2001) described the Falcon AGG technology, while Lee et al (2006) described the introduction of the HeliFalcon AGG technology. Christensen et al (2015) presented a detailed analysis of noise and repeatability of Falcon AGG data, and a comparison with high resolution ground gravity data.

The HeliFalcon AGG system, as deployed on a geothermal survey in Japan, is shown in Fig.1. In addition to gravity data, the system acquires DGPS navigational and positional data, and high-resolution laser scanner DTM data which is used to calculate rigorous terrain corrections for the gravity data. The system can also be configured to simultaneously acquire stinger magnetics if required.

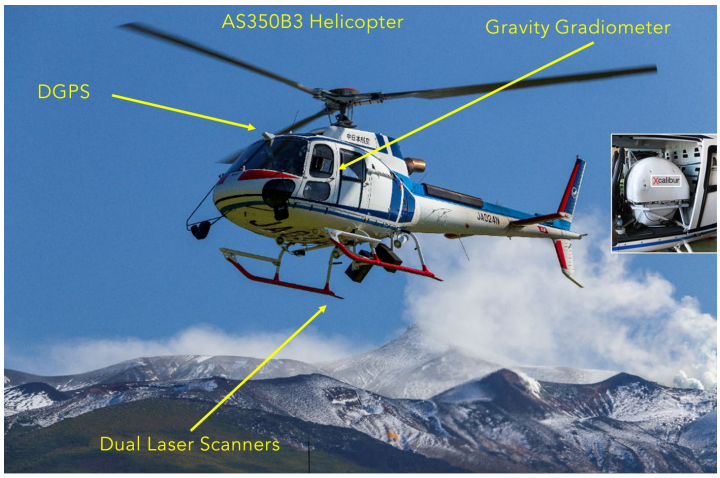

Figure 1: The HeliFalcon airborne gravity gradiometry system on survey in Hokkaido, Japan.

HELITEM^2 Airborne Electromagnetics and Magnetics

Helitem^2 is a time domain electromagnetic system which acquires high resolution electromagnetic and magnetic data. Smiarowski (2020) described the Helitem^2 system. See Fig. 2.

Helitem^2 is designed for maximum depth of exploration and sensitivity to target, and features:
- coincident geometry
- a large diameter transmitter loop - 35m
- high-power square waveform transmitter – (560,000Am^2)
- transmitter frequencies - 6.25, 12.5 or 25Hz
- large diameter, low-noise receiver – 3 component

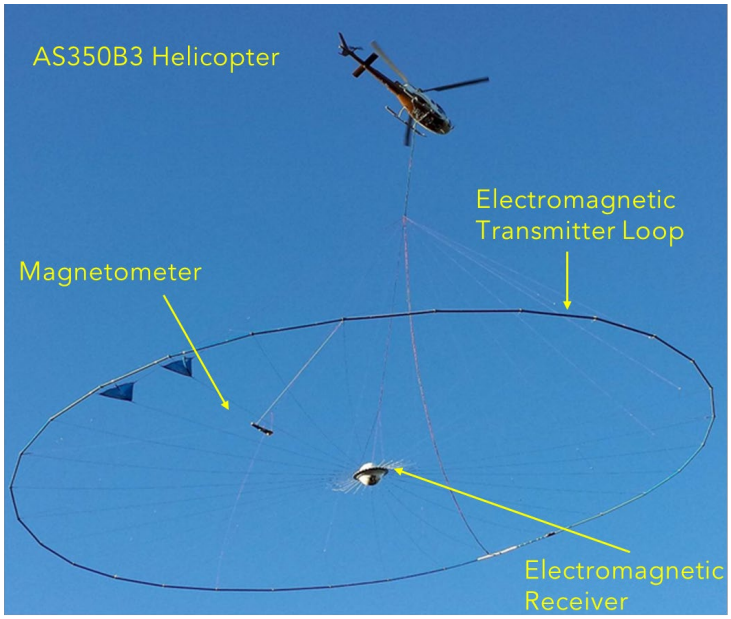

Figure 2: The Helitem^2 electromagnetic and magnetic EM system.

ACQUIRED AIRBORNE GEOPHYSICAL DATASETS

In total, 9,932 line-km of HeliFalcon AGG data and 5,567 line-km of Helitem AEM and magnetic data were acquired.

The acquired datasets are shown in Figs. 3, 4 and 5.

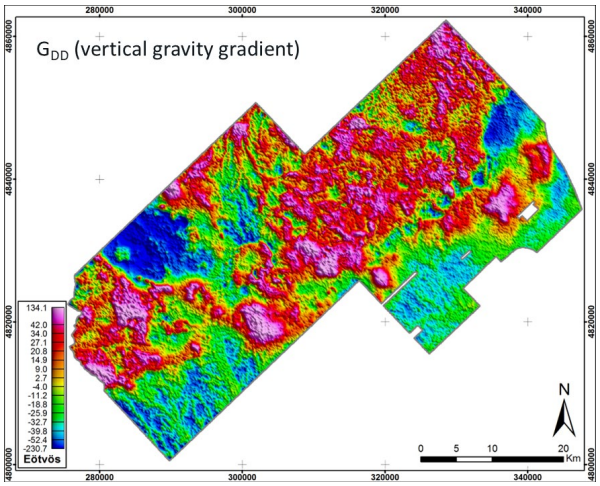

Figure 3: HeliFalcon AGG Data – Vertical Gravity Gradient (GDD)

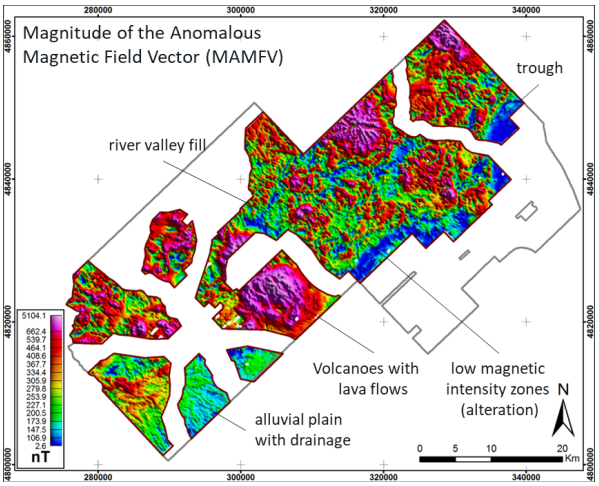

Figure 4: Magnetic Data – Magnitude of the Anomalous Magnetic Field Vector (MAMFV)

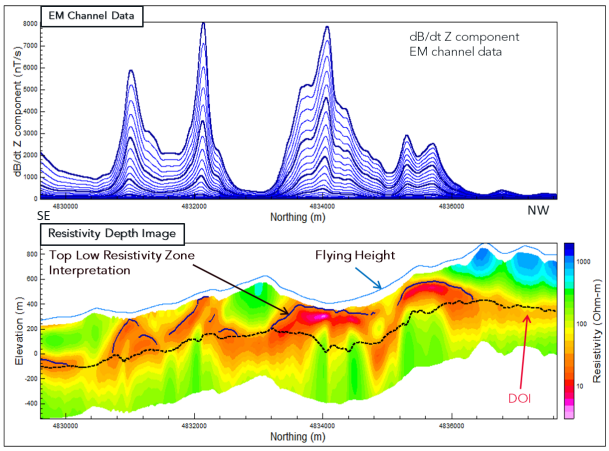

Figure 5: Helitem AEM Data – Resistivity Depth Image (UBC 1DTM)

INTEGRATED INTERPRETATION

Initially the regional geological setting was investigated using public domain data. Then interpretation of the Gravity Gradient, Magnetic and EM data were undertaken individually. Finally, all the individual interpretations were integrated. Figures 6, 7 and 8 show the integrated interpretation displayed on backgrounds of gravity, magnetic and electromagnetic data respectively.

Lithologies and structures were mapped in ArcGIS. Both lineaments and concentric boundaries were mapped, with the latter interpreted to be caldera ring faults. Structures identified from the AGG and magnetic data are consistent with the previously known faults, while the high resolution of the newly acquired data resulted in the detailed mapping of a significant additional number of new tectonic and volcanic structures.

The structural interpretation of the Musadake area (NE) of the block shows northeast structures. Major lineaments in the Teshikaga area (W) of the block trend west to west-southwest. These lineaments appear to offset the older northeast trend. Continuous northwest to north trending structures are important, particularly in the Musadake area, and may represent a subvertical conjugate fault system formed as a result of northwest compression across the area. The northwest to north trending faults may provide important conduits where they intersect one another, and where they intersect the northeast-striking faults (e.g. at Musadake volcano).

The timing of volcanism in the Musadake and Teshikaga areas appears directly related to the tectonic age of the mapped lineaments. In the Musadake area, volcanism is predominantly of Miocene to Pleistocene in age. In the Teshikaga area, younger volcanism associated with west to southwest trending faults is dated between the Pleistocene and Recent epochs.

The rhombic shape of the volcanic structures in the Teshikaga area, defined by the lineament interpretation from all datasets, suggests a pull-apart setting. See marked C on Fig. 12.

Low resistivity zones were interpreted using the AEM data, both in map form and on resistivity depth sections. These low resistivity zones, which may indicate the presence of clays associated with hydrothermal alteration, are commonly associated with discrete magnetic lows in the magnetic maps. The reduced magnetic susceptibilities may reflect thermal destruction of magnetite and/or chemical alteration processes such as the conversion of magnetite to pyrite.

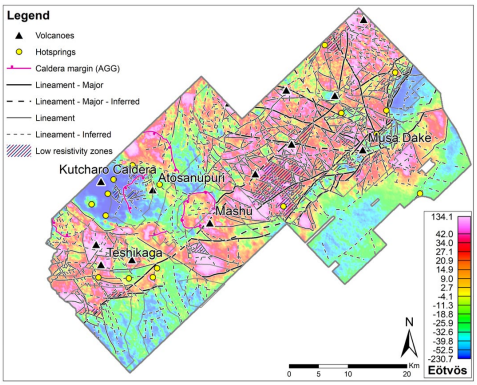

Figure 6: Integrated Interpretation on AGG Vertical Gravity Gradient Data (G_{DD})

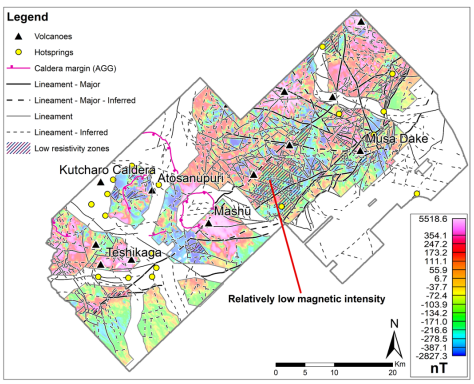

Figure 7: Integrated Interpretation on Magnetic Data (differential RTP of the Residual Magnetic Intensity)

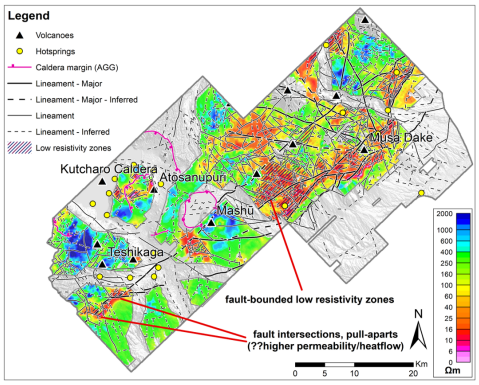

Figure 8: Integrated Interpretation on a Resistivity Depth Slice at 100m above mean sea level

Further Analysis of the Electromagnetic Data

To better understand of the 3D resistivity distribution in the survey area, inversions were run on the Helitem data using UBC's 1DTM inversion code. Resistivity Depth Images were generated for all survey lines, as shown previously in Fig.5.

A 3D resistivity voxel model, shown in Fig. 9, was calculated from the RDI profiles, by interpolating between the profiles using a minimum curvature 3D gridding algorithm.

The 3D Voxel model was then used to extract resistivity depth slices (See Fig.8), and data subsets including the resistivity iso-surface shown in Fig 10., which displays the lower resistivity (<25 Ωm) volumes within the model to visualize the 3D distribution of the more conductive rocks, interpreted as the low resistivity zones. These zones include abundant clay caps, and indicate geothermal potential.

Other parameters derived from the 3D resistivity voxel model includes 3D surface estimates of the depth to the top of the low resistivity zone. See Fig. 11.

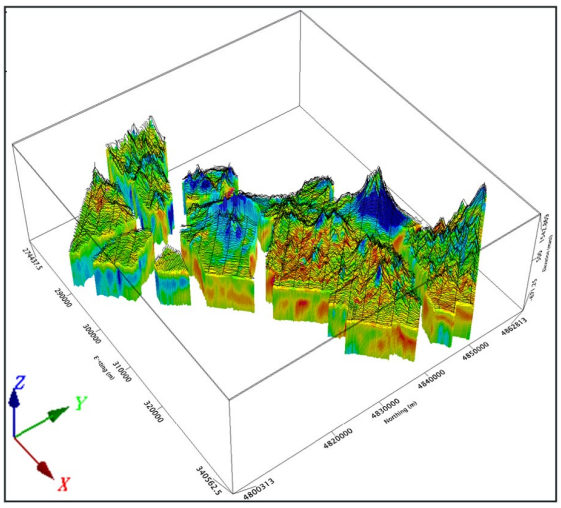

Figure 9: 3D Resistivity Voxel Model

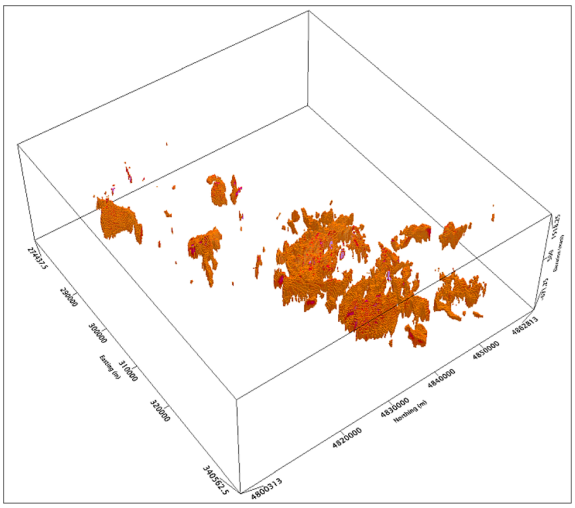

Figure 10: 3D Resistivity Voxel (25 Ωm) Iso-Surface of Interpreted Low Resistivity (Clay-Cap) Zone

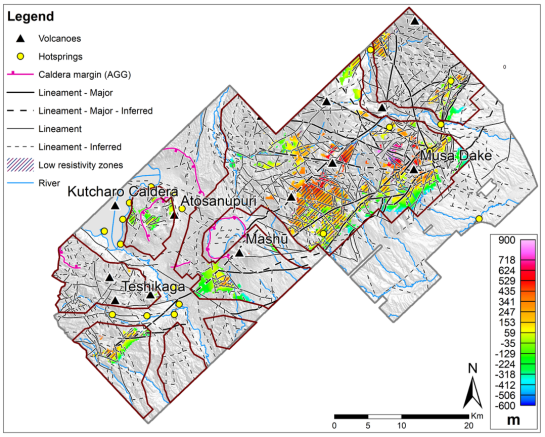

Figure 11: Interpreted Depth of the Top of the Low Resistivity Zone above mean sea level

Geothermal Prospectivity

On completion of the integrated interpretation, a brief analysis was conducted to identify potentially prospective geothermal areas for further study. The prospective areas identified from the acquired data coincide with low resistivity zones across the Musadake-Teshikaga survey area.

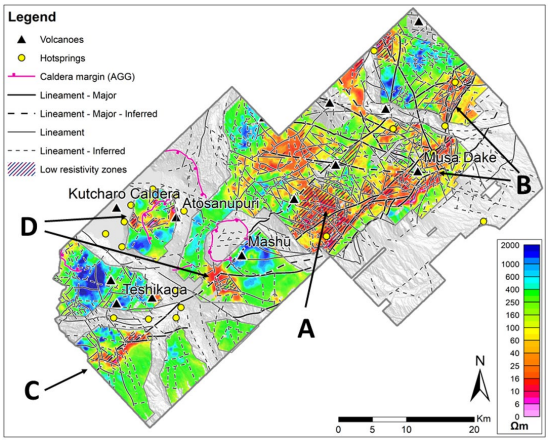

Figure 12: Resistivity at 100m above mean sea level, marked with geothermally prospective areas.

The largest low resistivity zone is in the central-southwest of the Musadake area, marked A on Fig. 12.

Elongate northeast trending low resistivity zones are also present north and south of Musadake (B on Fig. 12) and southwest of Teshikaga (C on Fig. 12). These conductive zones appear to occur along major northeast trending structures through the survey area.

Smaller isolated low resistivity zones are present west of the Atosanupuri Volcano and southwest of Maschū Volcano. (D on Fig. 12). Hotsprings and fumaroles are abundant around these lakes, as well as along northeast lineaments interpreted across the survey area.

The low resistivity zones across the area are structurally well-defined in the AGG, magnetic and AEM data. Observed low magnetic intensities in these areas may be related to destruction of magnetite from hydrothermal activity.

Integrated interpretation of multiple datasets reduces ambiguity in geothermal exploration. There is often a good relationship between features mapped from the airborne gravity, resistivity, and magnetic data, as the lithological distribution and alteration is controlled by tectonic and volcanic structures.

CONCLUSIONS

HeliFalcon AGG and Helitem AEM technologies have been used to acquire high resolution gravity, resistivity, and magnetic datasets in challenging terrain.

Structures identified from AGG data are consistent with the known faults, while abundant additional tectonic and volcanic structure could be mapped in detail using the higher resolution airborne gravity gradiometry data.

Low resistivity zones are generally well constrained by the mapped lineaments, and most are interpreted as zones of hydrothermal alteration and considered prospective. The top of these low resistivity zones could be identified by Resistivity Depth Imaging.

Some low resistivity areas coincide with areas of reduced magnetic susceptibility interpreted to be due to the thermal and alteration effects on magnetite.

Integrated interpretation of multiple datasets reduces ambiguity in geothermal exploration. There is often a good relationship between features mapped from the airborne gravity, resistivity, and magnetic data, as the lithological distribution and alteration is controlled by tectonic and volcanic structures.

The data acquired in the Musadake-Teshikaga area has proven to be of significant value for geothermal exploration and assessment.

ACKNOWLEDGMENTS

The authors thank Japan Oil, Gas and Metals National Corporation (JOGMEC) for previously allowing use of the Musadake-Teshikaga datasets.

REFERENCES

Christensen, A.N., Dransfield, M.H., and Van Galder, C., Noise and repeatability of airborne gravity gradiometry, EAGE First Break Vol. 33, pp 55 – 63, April 2015

Lee, J.B., Boggs, D.B., Downey, M.A., Maddever, R.A.M., Turner, R.J. and Dransfield, M.H., First test survey results from the FALCON™ helicopter-borne airborne gravity gradiometer system, Australian Earth Sciences Conference, Melbourne, Australia, July 2006

Lee, J.B., FALCON gravity gradiometer technology, Exploration Geophysics 3, Vol. 32, No 3 & 4, pp 175 – 178, 2001

Smiarowski, A., New Technology in Airborne TEM for Deep and Covered Targets with Western Australian Examples, ASEG WA Branch Technical Presentation, August 2020

Van Galder, C., Dransfield, M., Full Spectrum Falcon – Improving AGG Quality at Both Ends of the Spectrum, Extended Abstracts, ASEG-PESA_AIG 2016